

# Quantum critical magnetotransport at a continuous metal-insulator transition

P. Haldar,<sup>1,\*</sup> M. S. Laad,<sup>1,†</sup> S. R. Hassan,<sup>1,‡</sup> Madhavi Chand,<sup>2,§</sup> and Pratap Raychaudhuri<sup>2,||</sup>

<sup>1</sup>*Institute of Mathematical Sciences, Taramani, Chennai 600113, India and Homi Bhabha National Institute Training School Complex, Anushakti Nagar, Mumbai 400085, India*

<sup>2</sup>*Tata Institute of Fundamental Research, Homi Bhabha Rd, Colaba, Mumbai 400005, India*

(Received 27 June 2016; revised manuscript received 12 July 2017; published 10 October 2017)

In contrast to the seminal weak localization prediction of a noncritical Hall constant ( $R_H$ ) at the Anderson metal-insulator transition (MIT),  $R_H$  in quite a few real disordered systems exhibits both a strong  $T$  dependence and critical scaling near their MIT. Here we investigate these issues in detail within a nonperturbative “strong localization” regime using cluster-dynamical mean-field theory (CDMFT). We uncover (i) clear and unconventional quantum-critical scaling of the Gell-Mann law, or  $\gamma$  function for magnetotransport, finding that  $\gamma(g_{xy}) = \frac{d[\log(g_{xy})]}{d[\log(T)]} \simeq \log(g_{xy})$  over a wide range spanning the continuous MIT, very similar to that seen for the longitudinal conductivity, and (ii) strongly  $T$  dependent and clear quantum critical scaling in both transverse conductivity and  $R_H$  at the MIT. We show that these surprising results are in comprehensive and very good accord with signatures of a novel Mott-like localization in NbN near the MIT, providing substantial support for our “strong” localization view.

DOI: 10.1103/PhysRevB.96.155113

## I. INTRODUCTION

At low temperatures ( $T$ ), transport in normal metals arises as a result of scattering of weakly interacting fermionic (Landau) quasiparticles amongst themselves, phonons, and impurities [1]. Remarkably, it seems to hold even for  $f$ -electron systems, which are certainly strongly correlated Fermi liquids. However, this appealing quasiclassical description fails near metal-insulator transitions (MITs), where the Landau quasiparticle description itself breaks down [2]. In fact, in cuprates [3] and some  $f$ -electron systems [4], resistivity and Hall data can only be reconciled by postulating *two* distinct relaxation rates, arising from the breakup of an electron, for the decay of longitudinal and transverse currents. In many cases, bad-metallic and linear-in- $T$  resistivities preclude use of Boltzmann transport views altogether, since the picture of weakly interacting Landau quasiparticles itself breaks down.

In disorder-driven MITs, resistivity and Hall effect have long been studied in the context of the seminal weak-localization (WL) theory [5]. These studies already threw up interesting hints regarding the inadequacy of WL approach upon attempts to reconcile criticality in (magneto)transport [6]. Specifically, while both  $\sigma_{xx}(n) \simeq (n_c - n)^\nu$  and  $\sigma_{xy}(n) \simeq (n_c - n)^{\nu'}$  turned out to be critical at the MIT, and the ratio  $\nu'/\nu \simeq 1$  in stark contrast to the value of 2 predicted at the Anderson MIT [7]. More recent work on intentionally disordered NbN [8], wherein the system is driven across  $k_F l \simeq O(1)$  (here  $k_F$  is the Fermi wave vector and  $l$  is the mean-free path, and  $k_F l \gg 1$  describes a good metal, while  $k_F l \leq 1.0$  describes a bad metal without well-defined electronic quasiparticles), shows clear signatures of an unusual type of localization at odds with theoretical predictions if one insists on an Anderson disorder-driven MIT: (i)  $\rho_{xx}(T) \simeq$

$C + AR_H(T)$ , both increasing with reduction in  $T$  over a wide range of  $k_F l$  far *before* the MIT occurs [in NbN, this is pre-empted by a superconductor-insulator transition (SIT) [8] at very low  $T$  near the critical  $(k_F l)_c$ ], and (ii)  $\Delta R_H/R_H \simeq 0.69[\Delta\rho_{xx}(T)/\rho_{xx}]$ , widely different from  $\Delta R_H/R_H \simeq 2.0[\Delta\rho_{xx}(T)/\rho_{xx}]$  expected to hold in WL theory [9] ( $k_F l \gg 1$ ). These anomalies in both  $\rho_{xx}$  and  $R_H(T)$  are inexplicable within WL views (where  $R_H$  is  $T$  independent and *noncritical* at the MIT), and point toward a fundamentally new mechanism at work. Two possible reasons for this discord are: (1) electron-electron ( $e$ - $e$ ) interactions grow [10] near a disorder-induced MIT and may destroy the one-electron picture, and/or (2) such experiments maybe probing the “strong” localization regime of a disorder problem, where nonperturbative strong scattering effects may also destroy the one-electron picture. This is because Boltzmann approaches are untenable at the outset when  $k_F l \simeq 1$ , when a quasiparticle view itself breaks down.

Motivated by the above issues, we investigate magneto-transport near a *continuous* (at  $T = 0$ ) MIT. We choose the Falicov-Kimball model (FKM) because (i) it is the simplest model of correlated fermions exhibiting a continuous MIT, (ii) is *exactly* soluble within (cluster) dynamical mean-field theory [(C)DMFT] for arbitrarily strong interaction, and (iii) a two-site cluster DMFT treats the all-important short-range correlations precisely on the length scale of  $l \simeq k_F^{-1}$ . Moreover, it is isomorphic to the binary-alloy Anderson disorder model, except that the FKM has *annealed* instead of quenched disorder.

## II. CALCULATION OF DC CONDUCTIVITY TENSOR WITHIN CLUSTER DMFT

The Hamiltonian of the spinless FKM is

$$H_{\text{FKM}} = -t \sum_{\langle i,j \rangle} (c_i^\dagger c_j + \text{H.c.}) + U \sum_i n_{i,d} n_{i,c} + \mu \sum_i n_{i,c} \quad (1)$$

on a Bethe lattice with a semicircular band density of states (DOS) as an approximation to a  $D = 3$  lattice.  $c_i, c_i^\dagger, d_i, d_i^\dagger$  are

\*prosenjit@imsc.res.in

†mslaad@imsc.res.in

‡shassan@imsc.res.in

§madhavichand2009@gmail.com

||pratap@tifr.res.in

fermion operators in dispersive band ( $c$ ) and dispersionless ( $d$ ) states,  $t$  is the one-electron hopping integral, and  $U$  is the on-site repulsion for a site-local doubly occupied configuration. Since  $n_{i,d} = 0, 1$ ,  $v_i = Un_{i,d}$  is also viewed as a static but *annealed* “disorder” potential for the  $c$  fermions. We take noninteracting  $c$  fermions half-bandwidth as unity, i.e.,  $2t = 1$ .

As studied earlier for the dc resistivity [11], we now use the exact-to- $O(1/D)$  cluster propagators  $G_{\mathbf{K}}(\omega)$  for each of the two-site cluster momenta  $\mathbf{K} = (0,0), (\pi,\pi)$  to compute the full conductivity tensor  $\sigma_{ab}(T)$ , with  $a, b = x, y$ . We neglect the vertex corrections to the Bethe-Salpeter equation (BSE) for all the intracenter momenta since they are negligible even within CDMFT, as can be seen, for example, within a cluster-to-orbital mapping [12,13]. Thus, this constitutes an excellent approximation for computation of transport coefficients. Explicitly, the dc conductivity reads

$$\sigma_{xx}(T) = \sigma_0 \sum_{\mathbf{K}} \int_{-\infty}^{+\infty} d\epsilon v^2(\epsilon) \rho_0^{\mathbf{K}}(\epsilon) \times \int_{-\infty}^{+\infty} d\omega A_{\mathbf{K}}^2(\epsilon, \omega) \left( \frac{-df}{d\omega} \right), \quad (2)$$

where  $\sigma_0 = \frac{\pi e^2}{\hbar D a} \simeq (10^{-3} - 10^{-2})(2/D)$  ( $\mu\Omega$ )  $\text{cm}^{-1}$ ,  $\rho_0^{\mathbf{K}}(E)$  is the “partial” unperturbed DOS used in earlier work [14], and  $A_{\mathbf{K}}(E)$  is the intracenter CDMFT one-fermion spectral function. The Hall conductivity is a more delicate quantity to compute [15]. Fortunately, absence of vertex corrections comes to the rescue and we find

$$\sigma_{xy}(T) = \sigma_{xy,0} B \sum_{\mathbf{K}} \int d\epsilon v^2(\epsilon) \rho_0^{\mathbf{K}}(\epsilon) \epsilon \times \int d\omega A_{\mathbf{K}}^3(\epsilon, \omega) \left( \frac{df}{d\omega} \right), \quad (3)$$

with  $\sigma_{xy,0} = -\frac{2\pi^2 |e|^3 a}{3\hbar^2} (1/2D^2)$ , and  $B$  is the magnetic field. Now, the Hall constant is simply  $R_H(T) = \frac{\sigma_{xy}}{B\sigma_{xx}^2}$  and the Hall angle is  $\cot\theta_H = \frac{\sigma_{xx}}{\sigma_{xy}}$ . We show the off-diagonal conductivity  $\sigma_{xy}(U, T)$  as a function of  $U$  from small to large  $U$  across the continuous MIT occurring at  $U_c = 1.8$  [14]. First, we show results for the temperature-dependent off-diagonal conductivity  $\sigma_{xy}(T)$  as a function of  $U$  across the continuous Mott transition.

### III. RESULTS AND DISCUSSIONS

We use Eq. (3) to compute  $\sigma_{xy}(T, U)$ . In Fig. 1 we show  $\sigma_{xy}(T, U)$  as a function of temperature ( $T$ ) for different disorder values ( $U$ ). A clear change of slope at low  $T < 0.05t$  occurs around  $U \simeq 1.3$ , which seems to correlate with the bad-metal-to-bad-insulator crossover in the dc resistivity in our earlier study [11]. Close to the MIT,  $\rho_{dc}(T)$  diverges approximately like  $\exp(E_g/k_B T)$  as  $T \rightarrow 0$  in this regime,  $R_H(T \rightarrow 0)$  diverges as it must, since the MIT is accompanied by loss of carriers due to gap opening. A clear change of slope (for  $T < 0.05t$ ) occurs around  $U = 1.3$ , and  $\sigma_{xy}(T) \simeq T^{1.2}$  around  $U_c$ . The dc resistivity  $\rho_{xx}(T)$  shows extremely bad-metallic behavior at lowest  $T$ , beautiful mirror symmetry, and novel “Mott-like” scaling [11] precisely in this regime. It is obviously of interest to inquire whether the novel features seen in  $\rho_{xx}(U, T)$  are also reflected in magnetotransport

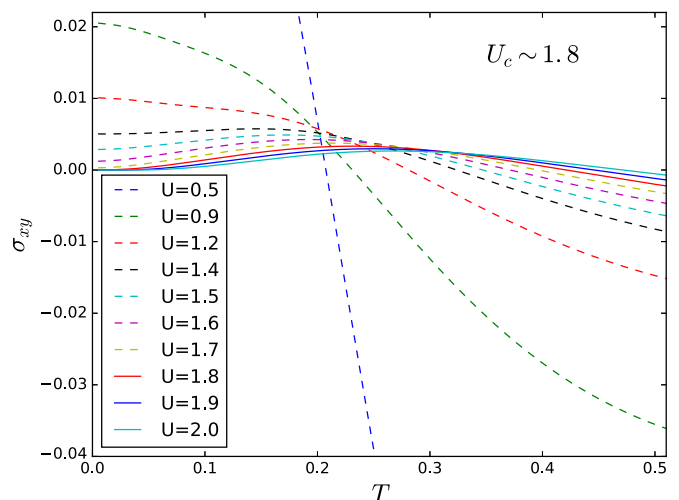


FIG. 1. Hall conductivity ( $\sigma_{xy}$ ) as a function of temperature ( $T$ ) for different  $U$ .

near the “Mott” QCP. To facilitate this possibility, we show  $\log_{10}(\frac{\sigma_c^{xy}}{\sigma_{xy}(T)})$  versus  $T$  in the left panel of Fig. 2, finding that the family of  $1/\sigma^{xy}(U, T)$  curves also exhibit a near-perfect “mirror” symmetry over an extended region around  $1/\sigma_c^{xy}(U, T)$ , strongly presaging quantum critical behavior.

To unearth this feature, we also show  $\log_{10}(\frac{\sigma_c^{xy}}{\sigma_{xy}(T)})$  versus  $T/T_0^{xy}$  in the right panel of Fig. 2, where we have repeated the unbiased method of introducing a  $T_0^{xy}(U)$  to rescale all metallic and insulating curves on to two universal curves. Remarkably, as for the  $\rho_{xx}$  scaling, we find, as shown in the left panel of Fig. 3, that  $T_0^{xy}$  vanishes precisely at the MIT. Clear scaling behavior we find testifies to a remarkable fact: the novel scaling features found earlier in dc resistivity are also clearly manifest in the off-diagonal resistivity.

Even clearer characterization of the quantum critical features is obtained when we compute the  $\gamma$  function [7] (this is

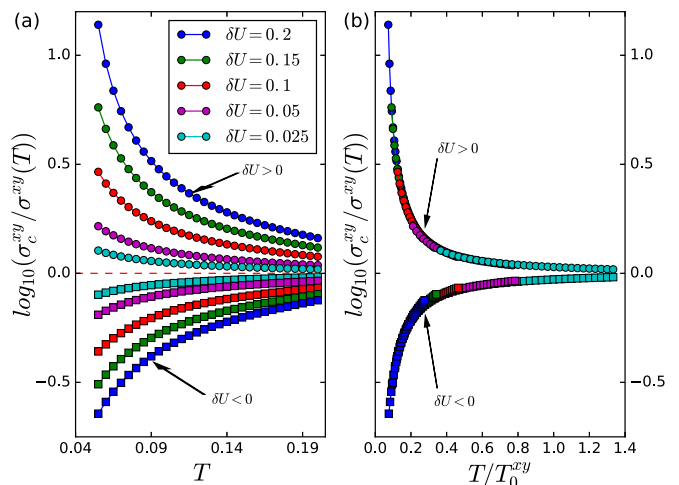


FIG. 2. (a) In the left panel,  $\log_{10}(\frac{\sigma_c^{xy}}{\sigma_{xy}(T)})$  as a function of temperature  $T$  for  $\delta U = \pm 0.025, 0.05, 0.1, 0.15, 0.2$ ;  $\sigma_c^{xy}$  is the “separatrix.” (b) In the right panel, scaling the data along  $T$  axis by scaled temperature  $T_0^{xy}$ .

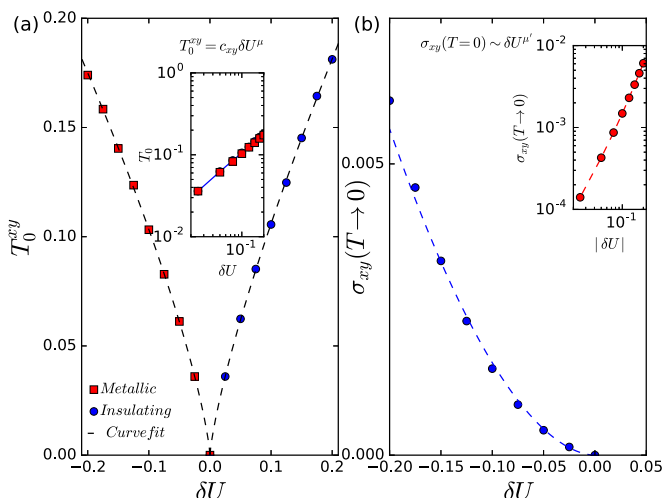


FIG. 3. (a) In the left panel, scaling parameter  $T_0^{xy}$  as a function of control parameter  $\delta U = U - U_c$ ; the inset illustrates power-law dependence of scaling parameter  $T_0^{xy} = c |\delta U|^\mu$ . (b) In the right panel,  $\sigma_{xy}(T \rightarrow 0)$  as a function of control parameter  $\delta U = U - U_c$ ; the inset illustrates power-law dependence of  $\sigma_{xy}(T \rightarrow 0) = c |\delta U|^{\mu'}$ .

the analog of the well-known  $\beta$  function for the longitudinal conductivity) for  $\sigma_{xy}(U, T)$ , defined by  $\gamma(g_{xy}) = \frac{d[\ln(g_{xy})]}{d[\ln(T)]}$ , with  $g_{xy} = \sigma^{xy}(T)/\sigma_c^{xy}$ . As shown in Fig. 4, it is indeed remarkable that it clearly varies as  $\ln(g_{xy})$ , and is continuous through  $\delta U = 0$ . This shows that it has precisely the same form on both sides of the MIT, which is exactly the feature needed for genuine quantum criticality. These features resemble those found for QC scaling in  $\rho_{xx}$  [11], showing that, like  $\beta(g)$ ,  $\gamma(g_{xy}) \simeq \ln(g_{xy})$  deep into the metallic phase. Thus, we have found that the *full* dc conductivity tensor reflects the strong

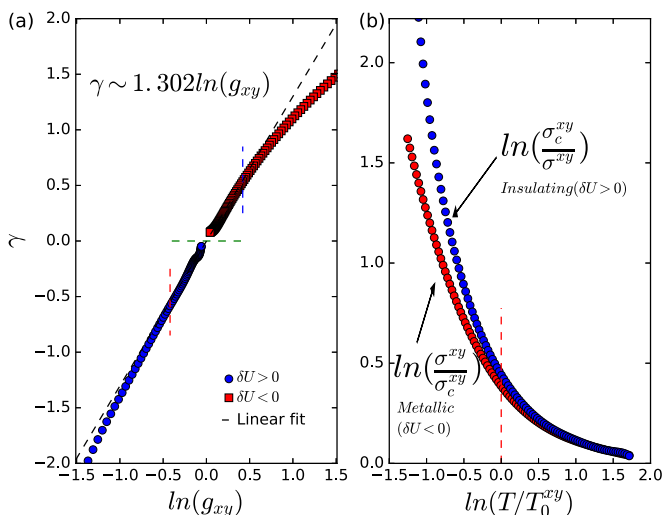


FIG. 4. (a) In the left panel,  $\gamma$  function shows linear  $\ln(g_{xy})$  behavior close to the transition. Squares are for the metallic branch ( $\delta U < 0$ ) and circles are for the insulating branch ( $\delta U > 0$ ); vertical dashed lines indicate the region where mirror symmetry of curves is found. (b) In the right panel, reflection symmetry of scaled curved close to the transition.

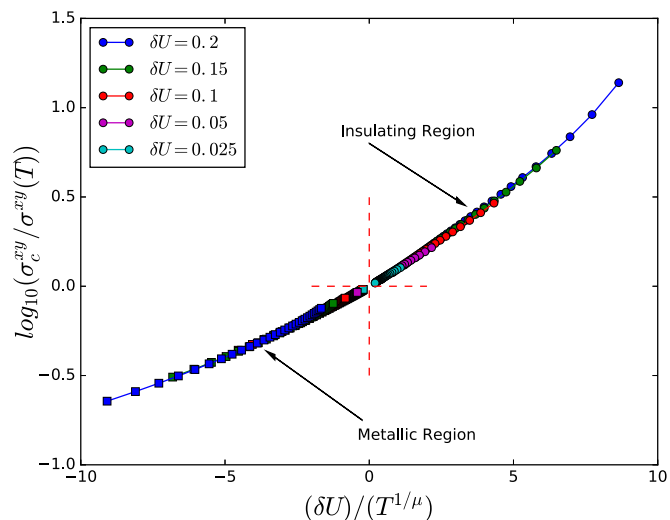


FIG. 5.  $\log_{10}(\frac{\sigma_c^{xy}}{\sigma^{xy}(T)})$  vs  $(\delta U)/T^{\frac{1}{\mu}}$ , where  $\delta U = U - U_c$ .

coupling nature of the Mott QCP, attesting to its underlying nonperturbative origin in Mott-like (strong scattering) physics.

That  $\gamma(g_{xy}) \simeq \ln g_{xy}$  holds on both sides of the MIT implies that its two branches must display “mirror symmetry” over an extended range of  $g_{xy}$ . In Fig. 4, left panel, we indeed see that magnetotransport around the QCP exhibits well-developed reflection symmetry (bounded by dashed vertical lines). It is also manifest in the right panel of Fig. 4, where  $\sigma_c^{xy}/\sigma^{xy}(\delta U) = \sigma^{xy}(-\delta U)/\sigma_c^{xy}$ ; i.e., they are mapped onto each other under reflection around  $U_c$ , precisely as found earlier for the dc resistivity. As a final check, we also show (see Fig. 5) that  $\log[\sigma_c^{xy}/\sigma^{xy}(T)]$  is a universal function of the “scaling variable”  $\delta U/T^{1/\mu}$ . Thus, our study explicitly shows the novel quantum criticality in magnetotransport at the Mott QCP (associated with a *continuous* Mott transition) in the FKM at strong coupling.

In an Anderson model framework, scaling of  $\sigma_{xy}$  is long known [7]. Our findings are very distinct from expectations for an Anderson-like transition: observe that we find  $T_0^{xy}(\delta U) \simeq c_{xy} |\delta U|^\mu$  (in the left panel of Fig. 3) with  $\mu \simeq 0.75 = 3/4$  (in the inset) on both sides of  $U_c$ , as required for genuinely quantum critical behavior. This strongly contrasts with the  $T_0^{xx}(\delta U) \simeq c |\delta U|^{z\nu}$  with  $z\nu = 1.32 \simeq 4/3$  found for the dc resistivity [11]. Furthermore, in the right panel of Fig. 3 we also show that  $\sigma_{xy} = \sigma_{0,xy}(U_c - U)^\mu$  with  $\mu' = 1.8$  (in the inset), quite distinct from  $\nu \simeq 4/3$  found earlier for  $\sigma_{xx}(U)$ .

Along with our finding of  $\sigma_{xx}(T) \simeq T$  and  $\sigma_{xy}(T) \simeq T^{1.2}$  at the MIT, these findings have very interesting consequences: (i) the Hall constant is critical at the MIT. We find  $R_H^{-1} \simeq \sigma_{xx}^2/\sigma_{xy} \simeq (U_c - U)^{0.8}$ , whereas  $R_H$  is noncritical [7] at the Anderson MIT. (ii)  $R_H$  is also strongly  $T$  dependent and divergent at the MIT, varying like  $R_H(T) \simeq T^{-0.8}$ , whereas  $R_H \simeq (nec)^{-1}$  in an Anderson disorder model. Concomitantly, the Hall angle also exhibits anomalous behavior: (iii)  $\tan\theta_H(T) \simeq T^{0.2}$  and  $\tan\theta_H(U) \simeq (U_c - U)^{1/2}$  in the quantum critical region. Our results are distinct from expectations from a Landau FL and Anderson-MIT views. At an Anderson MIT [7],  $R_H = (nec)^{-1}$  is  $T$  independent and noncritical at the MIT. In the metallic phase, use of semiclassical ideas dictates that *both*  $\beta(g)$  and  $\gamma(g_{xy})$  scale like  $(d - 2) - A/g$ , and the

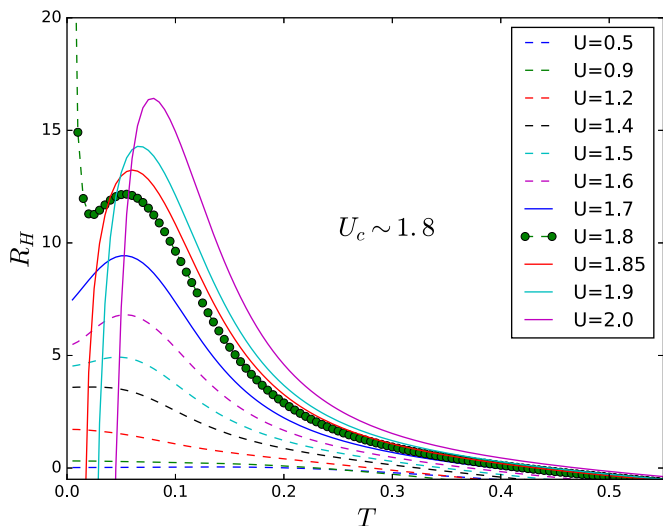


FIG. 6. Hall coefficient  $R_H$  as a function of temperature  $T$  for different  $U$ .

quantum correction to the Hall conductance is twice as big as for the Ohmic conductance. The stringent assumption under which this holds is that the inverse Hall constant [related to  $h(L) = L^{d-2}/R_H B$  in Abrahams *et al.*] scales classically like  $h(L) \simeq L^{d-2}$  for small  $B$  (large  $h$ ). It is precisely this assumption that breaks down when one considers the Mott MIT, where  $R_H$  is critical at the MIT (see above). They are also different from expectations in a correlated LFL: a strongly  $T$ -dependent  $R_H$  close to a Mott MIT in a Hubbard model framework is long known [16]. However, in a DMFT framework,  $R_H(T)$  exhibits a recovery of correlated Landau-Fermi liquid behavior below a low- $T$  lattice coherence scale. Moreover, in the MIT there is a first-order transition. In the FKM, the metallic state remains bad metallic and incoherent down to lowest  $T$ , and the MIT is continuous. The Mott-like character of the associated QCP is revealed by the observation of  $\beta(g) \simeq \log(g)$  and  $\gamma(g_{xy}) \simeq \log(g_{xy})$ .

In Fig. 6 we show  $R_H(U, T)$  versus temperature ( $T$ ). Both are indeed markedly  $T$  dependent. For an Anderson MIT,  $R_H$  would be noncritical. In a LFL metal, one expects  $\sigma_{xx}(T) = 1/\rho_{dc}(T) = AT^2$ , while  $\sigma_{xy}(T) \simeq T^{-4}$  at low  $T$ . In that case, we end up with a  $T$ -independent  $R_H$  and  $\cot\theta_H(T) = cT^2$ . This is the expected behavior for a LFL, where a single relaxation rate governs the  $T$ -dependent relaxation of longitudinal and Hall currents. The very different  $T$  dependencies we find here testify to the breakdown of this intimate link between LFL quasiparticles and this conventional behavior, and that the results we find are direct consequences of the destruction of LFL quasiparticles at strong coupling. They render semiclassical Boltzmann arguments (based on validity of  $k_F l \gg 1$ ) inapplicable at the outset.

#### IV. COMPARISON WITH EXPERIMENTAL RESULTS

We now turn to experiments to investigate how our theory stands this stringent test. Recent work on NbN [8] most clearly reveals ill-understood signatures of localization incompatible with weak localization predictions. In NbN, the effect of intentional charge disorder is to cause a random variation in

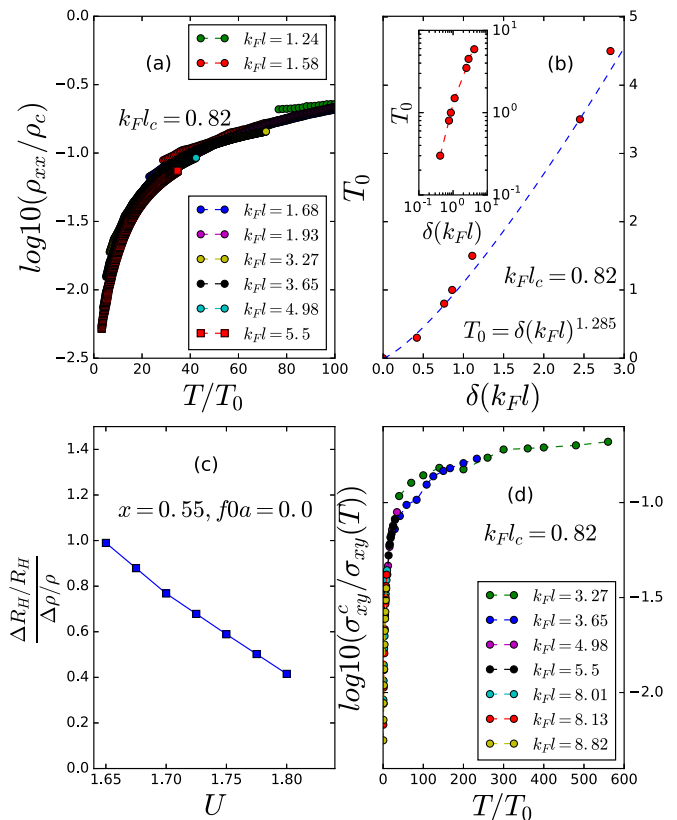


FIG. 7. (a) Resistivity data from Chand *et al.* [8], replotted as  $\log[\rho_{xx}(T)/\rho_c]$  versus  $T/T_0$  with  $T_0(\delta k_F l) \simeq |\delta k_F l|^{1.3}$  in (b), in excellent accord with theory [11]. In (c) we show that the theoretical ratio  $\frac{\Delta R_H/R_H}{\Delta \rho/\rho}$  is in the range of 0.5–0.7 near the Mott QCP, again in good qualitative accord with the value of 0.69 from Hall data [8]. In (d) we show clear scaling of the experimentally extracted  $\log[\sigma_{xy}^{(c)}/\sigma_{xy}(T)]$  in very good accord with theory for the same sample set used for (a). The  $\sigma_{xy}(T)$  is constructed from the experimental dc resistivity and Hall constant ( $R_H$ ). The  $R_H$  at the critical  $k_F l$  is calculated from extrapolation of the experimental Hall constant ( $R_H$ ) down to  $(k_F l)_c = 0.82$ , as shown in Fig. 8.

the local atomic potential, which increases as  $k_F l$  is reduced by increasing the disorder level. Following Freericks *et al.* [17], we posit that the FKM is a suitable effective model for materials like Ta<sub>x</sub>N and Nb<sub>x</sub>N, where carriers interact locally with randomly distributed charge disorder. We have reanalyzed Chand *et al.*'s data on NbN in light of the above results to test how our strong coupling view performs relative to data. To make meaningful contact with data on NbN, we make a reasonable assumption that increasing  $U/t$  in the FKM corresponds to decreasing  $k_F l$ , since the scattering strength should increase with  $U/t$ , reducing  $k_F l$  to  $O(1)$  [8] near the MIT. We find, as shown in Fig. 7(a), that (i)  $\log[\rho_{xx}(T)/\rho_c]$  on the (bad) metallic side scales with  $T/T_0(k_F l)$  exactly as predicted by our theory [11]. Furthermore, the data analysis shows [Fig. 7(b)] that  $T_0(k_F l) \simeq [k_F l - (k_F l)_c]^{z\nu}$  with  $z\nu \simeq 1.3$ , again in excellent accord with theory if we identify decreasing  $k_F l$  with increasing  $U$  in our model. (ii) Interestingly, our  $\rho_{xx}(T), R_H(T)$  results reproduce the detailed  $T$  dependence seen in data [8] with only one adjustable parameter ( $U$ ). (iii) Even more remarkably, we find that  $(\Delta R_H/R_H)/(\Delta \rho_{xx}/\rho_{xx})$ ,

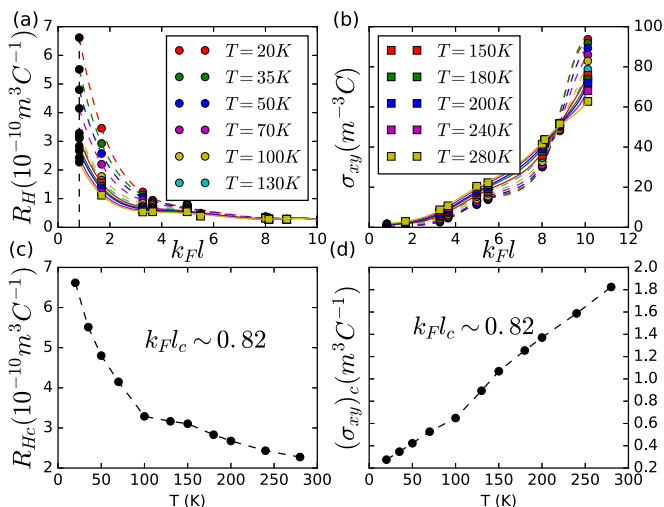


FIG. 8. (a) In the top-left panel, Hall constant  $R_H$  as a function of  $k_{Fl}$  for various temperature  $T$ , black circles are the values of  $R_H$  after extrapolating the curves up to critical  $k_{Fl} = 0.82$ . (b) In the top-right panel, Hall conductivity  $\sigma_{xy}$  calculated from the Hall constant ( $R_H$ ) and dc resistivity ( $\rho_{xx}$ ) as a function of  $k_{Fl}$  for various temperature  $T$ . (c) In the bottom-left panel, Hall constant  $R_H$  as a function temperature ( $T$ ) at the critical  $k_{Fl} = 0.82$  calculated from the extrapolation. (d) In the bottom-right panel, Hall conductivity  $\sigma_{xy}$  as a function temperature ( $T$ ) at the critical  $k_{Fl} = 0.82$ .

shown in Fig. 7(c), achieves values between 0.5 and 0.7 close to the MIT (between  $1.5 \leq U \leq 1.9$ ) in our model, in very good accord with 0.69 extracted in experiment. Finally, in Fig. 7(d), we uncover quantum critical scaling in  $1/\sigma_{xy}(T)$  as a function of  $k_{Fl}$  from data on NbN, which is expected in our model, since both  $\sigma_{xx}, \sigma_{xy}$  exhibit such novel scaling behavior. Since  $R_H$  is difficult to extract reliably in very bad-metallic samples (with  $k_{Fl} < 3.0$ ) close to the MIT, we resorted to a careful extrapolation of the Hall conductivity ( $\sigma_{xy}$ ) and Hall constant ( $R_H$ ) to smaller values of  $k_{Fl}$ .

In Fig. 8 we show the results of a careful fitting of the experimental data down to  $k_{Fl} \simeq O(1)$  [in fact, the critical

$(k_{Fl})_c$  is now consistent with 0.82, which is the critical value for the longitudinal dc conductivity]. Using these extrapolated fits to the dc conductivity tensor as a function of  $k_{Fl}$ , we constructed Fig. 7(d) in the main text. This makes our analysis consistent with a single  $(k_{Fl})_c \simeq 0.82$  for both  $\sigma_{xx}(k_{Fl}, T)$  and  $\sigma_{xy}(k_{Fl}, T)$ .

Taken together, earlier results of Chand *et al.* [8], now suitably reanalyzed in light of our CDMFT results, receive comprehensive explication within a strong localization view adopted here, lending substantial support to the view that the novel findings in NbN are representative of strong scattering effects near a continuous MIT, and involve microscopic processes beyond perturbative-in- $(1/k_{Fl})$  approaches.

#### IV. SUMMARY AND OUTLOOK

Thus, to conclude, we have presented clear evidence of novel quantum critical behavior in magnetotransport near a continuous MIT by a careful scaling analysis of CDMFT results for the off-diagonal conductivity for the FKM in the strong localization limit. We find that the loss of the quasi-particle pole structure at strong coupling ( $k_{Fl} \simeq 1$ ) leads to a rather distinct Mott-like quantum criticality, necessitating substantial modification of the quasiclassical Drude-Boltzmann transport schemes to study (magneto)transport. The resulting quantum criticality we find is closer to that expected from the opposite limit of strong localization based on a real-space locator expansion [18,19], as manifested in  $\gamma(g_{xy}) \simeq \ln(g_{xy})$ . Comprehensive and very good explication of recent data on NbN lend substantial experimental support to this Mott-like view. We suggest that strongly disordered electronic systems that show a bad-metallic resistivity and sizable  $T$ -dependent Hall constant would be promising candidates to unearth such novel quantum-critical magnetotransport at a continuous MIT. Finally, the similarity of QC scaling in resistivity in earlier work [11] to the Mott QC scaling in the Hubbard model [20] above the finite- $T$  critical endpoint suggests that related features discussed above may also manifest in wider classes of strongly correlated Mott materials.

- 
- [1] D. Pines and P. Nozieres, *Theory of Quantum Liquids* (Perseus Books, Cambridge, MA, 1999).
  - [2] M. Imada, A. Fujimori, and Y. Tokura, Metal-insulator transitions, *Rev. Mod. Phys.* **70**, 1039 (1998).
  - [3] T. R. Chien, Z. Z. Wang, and N. P. Ong, Effect of Zn Impurities on the Normal-State Hall Angle in Single-Crystal  $\text{YBa}_2\text{Cu}_{3-x}\text{Zn}_x\text{O}_{7-\delta}$ , *Phys. Rev. Lett.* **67**, 2088 (1991).
  - [4] S. Paschen, T. Lühmann, S. Wirth, P. Gegenwart, O. Trovarelli, C. Geibel, F. Steglich, P. Coleman, and Q. Si, Hall-effect evolution across a heavy-fermion quantum critical point, *Nature (London)* **432**, 881 (2004).
  - [5] P. A. Lee and T. V. Ramakrishnan, Disordered electronic systems, *Rev. Mod. Phys.* **57**, 287 (1985).
  - [6] S. B. Field and T. F. Rosenbaum, Critical Behavior of the Hall Conductivity at the Metal-Insulator Transition, *Phys. Rev. Lett.* **55**, 522 (1985).
  - [7] B. Shapiro and E. Abrahams, Scaling theory of the Hall effect in disordered electronic systems, *Phys. Rev. B* **24**, 4025 (1981).
  - [8] M. Chand, A. Mishra, Y. M. Xiong, A. Kamlapure, S. P. Chockalingam, J. Jesudasan, V. Bagwe, M. Mondal, P. W. Adams, V. Tripathi, and P. Raychaudhuri, Temperature dependence of resistivity and Hall coefficient in strongly disordered NbN thin films, *Phys. Rev. B* **80**, 134514 (2009).
  - [9] B. L. Altshuler, D. Khmel'nitzkii, A. I. Larkin, and P. A. Lee, Magnetoresistance and Hall effect in a disordered two-dimensional electron gas, *Phys. Rev. B* **22**, 5142 (1980).
  - [10] A. Punnoose and A. M. Finkel'stein, Metal-insulator transition in disordered two-dimensional electron systems, *Science* **310**, 289 (2005).
  - [11] P. Haldar, M. S. Laad, and S. R. Hassan, Quantum critical transport at a continuous metal-insulator transition, *Phys. Rev. B* **94**, 081115 (2016).

- [12] J. M. Tomczak and S. Biermann, Optical properties of correlated materials: Generalized Peierls approach and its application to VO<sub>2</sub>, *Phys. Rev. B* **80**, 085117 (2009).
- [13] K. Haule and G. Kotliar, Optical conductivity and kinetic energy of the superconducting state: A cluster dynamical mean field study, *Europhys. Lett.* **77**, 27007 (2007).
- [14] P. Haldar, M. S. Laad, and S. R. Hassan, Real-space cluster dynamical mean-field approach to the Falicov-Kimball model: An alloy-analogy approach, *Phys. Rev. B* **95**, 125116 (2017).
- [15] E. Lange, Memory-function approach to the Hall constant in strongly correlated electron systems, *Phys. Rev. B* **55**, 3907 (1997).
- [16] E. Lange and G. Kotliar, Magnetotransport in the doped Mott insulator, *Phys. Rev. B* **59**, 1800 (1999).
- [17] J. K. Freericks and V. Zlatić, Exact dynamical mean-field theory of the Falicov-Kimball model, *Rev. Mod. Phys.* **75**, 1333 (2003).
- [18] P. W. Anderson, Absence of diffusion in certain random lattices, *Phys. Rev.* **109**, 1492 (1958).
- [19] V. Dobrosavljević, E. Abrahams, E. Miranda, and S. Chakravarty, Scaling Theory of Two-Dimensional Metal-Insulator Transitions, *Phys. Rev. Lett.* **79**, 455 (1997).
- [20] H. Terletska, J. Vučićević, D. Tanasković, and V. Dobrosavljević, Quantum Critical Transport Near the Mott Transition, *Phys. Rev. Lett.* **107**, 026401 (2011).